

Snubber Circuit Application for Power-Factor Correction Flyback LED Driver

Burak Akin 

Department of Electrical Engineering, Yıldız Technical University, İstanbul, Turkey

Cite this article as: Akin B. Snubber Circuit Application for Power-Factor Correction Flyback LED Driver. *Electrica*, 2020; 20(1): 107-115.

ABSTRACT

Although there are basic, constant-current, buck, boost, and buck–boost type light-emitting diode (LED) drivers in the market, new LED drivers are being proposed in the literature. Owing to the development of the LED technology, the control problems associated with LED drivers have also occurred. Not only the pure control of LED drivers, but also the isolation and power-factor correction (PFC) demands are challenge for engineers. In this study, snubber circuits are added to the PFC flyback LED drivers to analyze the system in detail. To that end, the PAR230VEM application circuit is tested for its input and output parameters. The input and output waveforms of the PFC flyback LED driver are examined and compared with those of the other LED drivers in the literature. Subsequently, the proposed snubber circuits are added to the semiconductor components to improve the performance of the LED driver; this is because by adding the snubber circuits, the stress levels of the driver components are lowered. Consequently, the components with low stress levels improve the efficiency by approximately 9.4 %. Furthermore, the proposed isolated LED driver has unity power factor with 4.8 % THDi at the switching frequency of 69 kHz.

Keywords: Flyback, light-emitting diode (LED) driver, power-factor correction (PFC), snubber circuits

Corresponding Author:

Burak Akin

E-mail:

bakin@yildiz.edu.tr

Received: 24.12.2019

Accepted: 31.12.2019

DOI: 10.5152/electrica.2020.20093



Content of this journal is licensed under a Creative Commons Attribution-NonCommercial 4.0 International License.

Introduction

A light-emitting diode (LED) is a very small light source. It provides wide and easy-usage light in a short time with a long life up to 100,000 hours on average. There are billions of LEDs in the market, with their power ranging from several milli watts to high-power kilo watts. Sufficient current and voltage levels are required to be supplied to these LEDs; thus, power sources, which are called LED drivers, are required to be generated. Therefore, specific LED drivers have been developed and are often in the market. Furthermore, many LED-related studies exist in the literature [1-14]. However, these LED drives have to contain an increasing number of technological innovations. High efficiency, power-factor correction (PFC), and isolation are also mentioned when designing suitable drivers for LEDs.

Therefore, isolated LED driving circuits have been developed, and academic studies have been performed by researchers [15-16]. Owing to the low number of elements and economic use of flyback converters, they are also being studied for power below 150 W [17]. In addition, because of increasing interest in unity PFC circuits and soft switching techniques, improvements have been observed in this domain as well [18-23].

In this study, snubber circuits, which are based on passive soft switching technique, are added to the PFC flyback converter to realize the proposed LED driver. The circuit is analyzed with the added snubber circuit.

Flyback-Converter Design

A flyback converter functions on isolated buck–boost DC–DC converter operating principles. The rectified AC is controlled using a power switch via the primary side of the transformer. At that moment, the output load is fed by the output capacitor. When the energy is sufficient in

the primary side, the switching signal cuts, and, consequently, the primary-side energy is transferred to the output load. Therefore, the transformer is working as a coupled inductance rather than a transformer. The control signal is produced using a control IC, which is named LM3447 in Figure 1.

Therefore, if the secondary current falls to zero before the end of the Toff time, the circuit operates in the discontinuous current mode (DCM). However, if the current does not fall to zero within the aforementioned time, the circuit operates in the continuous current mode (CCM).

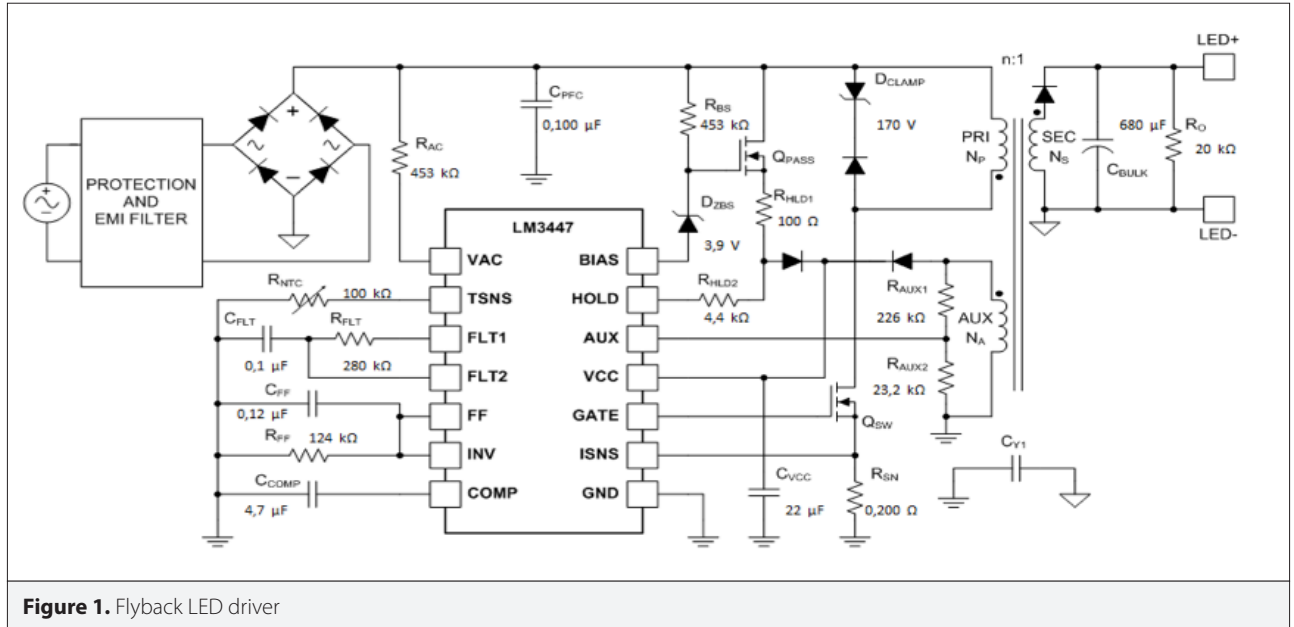


Figure 1. Flyback LED driver

The voltage drop on the power switch is subtracted from the input rectified voltage, V_{in} , to estimate the voltage level on the primary side of the transformer. This value is divided by the inductance, L_p , and multiplied by the T_{on} time of the control signal. Therefore, the primary-side current can be calculated as follows:

$$I_{PRI} = \frac{(V_{IN} - V_{DS(ON)}) * t_{ON}}{L_p} \quad (1)$$

When the control is cut, the T_{off} time begins, and the primary-side energy is transferred to the output load. In equation (2), the secondary-side current formula is written, where I_p denotes the primary-side current, N_p the number of primary turns, N_s the number of secondary turns, V_o the output voltage level, V_{d2} the voltage drop in diode D_2 , and T_{off} the off time of the control signal. One has the following:

$$I_{SEC} = \frac{I_p * N_s}{N_p} - \frac{(V_o + V_{D2}) * t_{OFF} * N_p^2}{N_s^2 * L_p}, I_{SEC} \geq 0 \quad (2)$$

To calculate the secondary current of the transformer, we must calculate the maximum value of the primary transferred current. Subsequently, this current decreases because of the power demand of the output load. The critical point is that if the secondary current falls to zero before the period ends, the output capacitor, C_{out} , again provides energy to the output load.

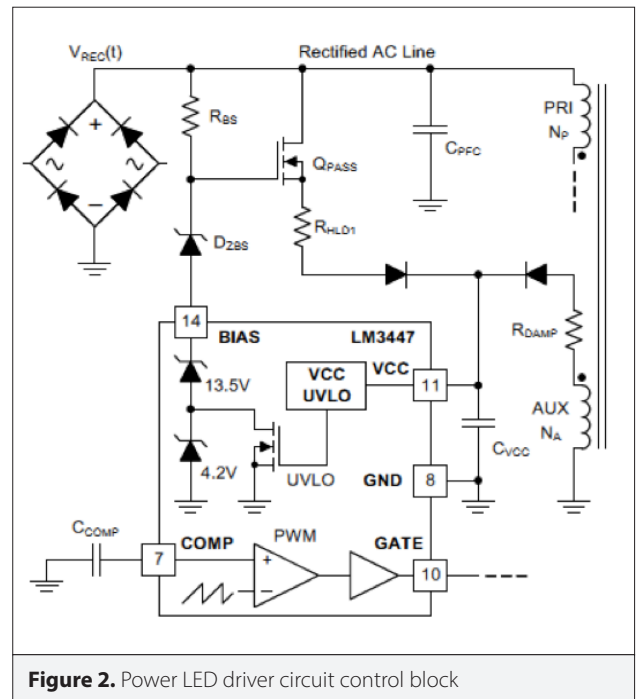


Figure 2. Power LED driver circuit control block

The output power can be calculated as in equation (3), where D denotes the duty (T_{on}/T_s), η the efficiency, and f_s the switching frequency. One has the following:

$$P_o = \frac{(V_{IN})^2 * D^2 * \eta}{2 * L_p * f_s} \quad (3)$$

The flyback converter is designed to provide the desired output values before they are required. For this requirement, the maximum and minimum values of both the input and output voltages, line frequency, switching frequency, output power, efficiency, control mode of the circuit, loss factor, and acceptable ripple factor or fluctuation values must be calculated.

The circuit operates depending on the internal structure of the LM3447 module. As depicted in Figure 2, it is designed for immediate drive operation using an external regulator circuit. At the startup, the bias voltage is controlled using the VCC low-current interlock circuit (UVLO). Subsequently, the rectified AC voltage is supplied to the bias via a resistor. A constant voltage of 17.7 V is applied to the bias so that the mosfet can quickly charge the capacitor. A resistance is used to limit the maximum operating current in the safe working zone for the mosfet.

The overcurrent protection mode of the LM3447 module protects the VCC from overvoltage ratings. The VCC threshold, 18.9 V, and 175-mV hysteresis comparator are monitored. After detecting the overvoltage, the GATE signal is lowered.

In the DCM, the PFC is performed as follows:

$$I_{P(PK)} = \frac{V_{REC}(t)}{L_M} * D * T_s = \frac{\|V_{in}(t)\|}{L_M} * D * T_s \quad (4)$$

$$V_{in}(t) = V_{IN(PK)} * \sin\left(\frac{2\pi}{T_L} * t\right) \quad (5)$$

If D is kept constant during a cycle, the peak value of the primary current changes in proportion to the input voltage. The input sinusoidal current can be calculated as follows:

$$i_{in}(t) = Average(I_p) \int_{T_s} = 0.5 * \frac{V_{in}(t)}{L_m} * D^2 * T_s \quad (6)$$

Consequently, the input average power can be calculated as follows:

$$P_{IN(AVG)} = \frac{2}{T_L} \int_0^{T_L} v_m(t) * i_m(t) * dt = \frac{2}{T_L} \int_0^{T_L} 0.5 * \frac{V_{IN(PK)}^2 * D^2 * T_s}{T_L} * \sin\left(\frac{2\pi}{T_L}\right) * dt \quad (7)$$

$$P_{IN(AVG)} = 0.25 * \frac{V_{IN(PK)}^2 * D^2 * T_s}{T_L} = \frac{V_{IN(RMS)}^2}{\left(\frac{2 * L_M}{D^2 * T_s}\right)}; R_c = \frac{2 * L_M}{D^2 * T_s} \quad (8)$$

Furthermore, the average LED current can be calculated as follows:

$$I_{LED(AVG)} = \frac{P_{OUT(AVG)}}{V_{OUT}} = \eta * \frac{P_{IN(AVG)}}{V_{OUT}} = \eta * \frac{V_{IN(RMS)}^2}{V_{OUT} * R_c} \quad (9)$$

The output LED current has two times more ripple content than that of the line frequency. Therefore, the output bulk capacitor must store sufficient energy in the Toff interval to limit twice the line-frequency fluctuation. The output capacitor value can be calculated as follows:

$$C_{BULK} \geq \frac{P_{IN}}{2\pi * f_L * R_{LED} * V_{OUT} * I_{LED(RIP)}} \quad (10)$$

Flyback Analysis

Flyback is a type of switch mode power supply (SMPS) to obtain an isolated buck-boost converter. The principal component of the circuits is a coupled transformer. Because the size of the transformer is directly proportional to the cost, the flyback circuits operate at high frequencies. Consequently, the high frequency increases the switching losses and also the noise in

Table 1. LED driver comparisons

Led Drivers	Input (V)	Input (A)	Cos φ	Output (V)	Output (A)	Input (W)	Output (W)
Low-cost ZVS [2]	218.8	0.0588	12.31	26.048	0.415	12.58	10.81
Open-loop CCM Mode [3]	110	0.132	5.7	42	0.285	14.458	12
Buck-Boost PFC [4]	220	0.07	12.04	40.26	0.314	15.19	12.67
CCM Boost [5]	220	0.43	7.69	80	1	94.12	80
Fix power controlled [6]	220	0.206	19.09	42.86	0.7	50.42	30
Flyback [7]	220	0.105	7.25	30	0.7	22.925	21
Dimmable [8]	218.7	0.102	5.13	68.4	0.276	22.21	18.18
Buck-Boost [9]	220	0.154	25.84	103.44	0.29	30.942	30
Soft-switched Buck [10]	220	0.105	2.56	29.7	0.707	23.08	21
Non-isolated Cuk [11]	230	0.152	35.11	31.64	0.703	28.59	22.25
Fourth-Order Buck [12]	110	0.38	5.56	24	1.25	41.8	30
High efficiency [13]	230	0.279	6.78	74	0.811	63.8	60
Low frequency [14]	220	0.103	5.13	69	0.28	22.57	19.32

Table 2. LED driver comparisons

Led Drivers	Efficiency (%)	Switching		PFC Yes/No	Isolation Yes/No	PF	THDi (%)
		Frequency (Hz)					
Low-cost ZVS [2]	86	48k		YES	NO	0.977	15
Open-loop CCM Mode [3]	83	50k		YES	NO	0.995	26.699
Buck–Boost PFC [4]	83.41	66k		YES	YES	0.978	19.96
CCM Boost [5]	85	40k		YES	YES	0.991	10
Fix power controlled [6]	85	25k		YES	YES	0.945	16.5
Flyback [7]	91.6	50k		YES	YES	0.992	12.6
Dimmable [8]	85	50k		YES	YES	0.996	1.61
Buck–Boost [9]	98.3	50k		YES	YES	0.9	4.38
Soft-switched Buck [10]	92	50k		YES	NO	0.999	2.6
Non-isolated Cuk [11]	77.82	50k		YES	NO	0.818	2.83
Fourth-Order Buck [12]	71.7	100k		YES	NO	0.995	6.2
High efficiency [13]	94	100k		YES	NO	0.993	8.22
Low frequency [14]	82.44	21.4k		YES	NO	0.996	3.19

the switching elements, whereas it decreases the volume of the transformer and cost. In recent years, flyback circuits have been preferred because of their low cost and low number of elements at medium and low power.

The LED drivers in the literature [2-14] are considered to examine their parameters. Therefore, in Table 1, the input voltage, input current, $\cos\phi$, output voltage, and output current and listed, and the corresponding output powers are presented for comparison.

The LED drivers in the literature [2-14] are compared with one another in Table 2 with respect to their efficiency, switching frequency, PFC, isolation, power factor (PF), and THDi.

- The low-cost ZVS LED driver circuit is not isolated, and it cannot prevent the harmonic from the grid; furthermore, its efficiency is low [2].
- The open-loop CCM mode LED driver circuit has high THDi and low efficiency, and it does not have isolation [3].
- The buck–boost PFC LED driver circuit has low efficiency and high THDi [4].
- The CCM boost LED driver has high output current, causing the LEDs to heat up and, consequently, shorten their lifetime [5].
- The constant-power-controlled LED driver has low efficiency and high THDi [6].
- The flyback LED driver is one of drivers with the highest efficiency; however, its THDi is high [7].
- The dimmable LED driver has acceptable PF and THDi values; however, its efficiency is low [8].
- The energy conversion buck–boost LED driver has high output voltage, which is above the optimum operating voltage [9].
- The soft-switched buck LED driver has its output at the desired values; however, there is no isolation [10].

- The isolated Cuk LED driver has low PF value [11].
- The fourth-order buck LED driver has no isolation [12].
- The high-efficiency buck LED driver has the best efficiency value. However, it has no isolation, and its output voltage is above the LED operating voltage [13].
- The output voltage of the low-frequency LED driver is considerably higher than the operating voltage, and it has no isolation [14].

Proposed PFC Flyback LED driver

To achieve PFC, the flyback LED driver PAR230VEM is used. The reference LED driver output voltage and current are 34 V and 350 mA, respectively. The initial output voltage and current waveforms are depicted in Figure 3. At the same time, the input voltage and current waveforms are depicted in Figure 4. Although the input voltage is in pure sinusoidal form, the shape of the current is distorted because of harmonics. Furthermore, the PF is far from the unity point.

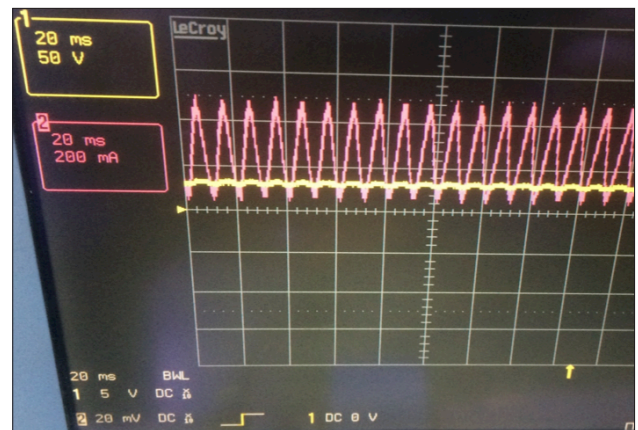


Figure 3. Output voltage and current waveforms

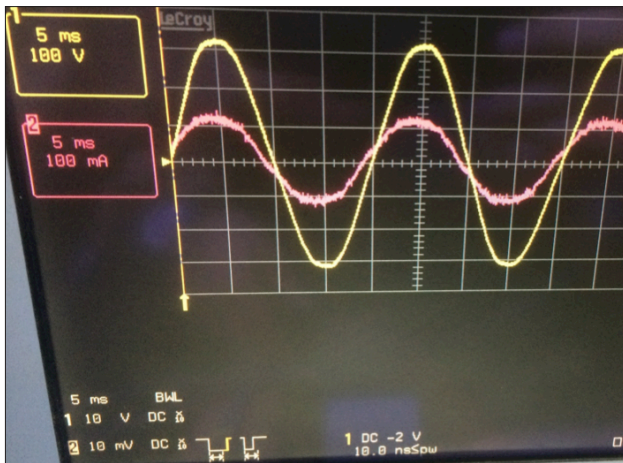


Figure 4. Input voltage and current waveforms

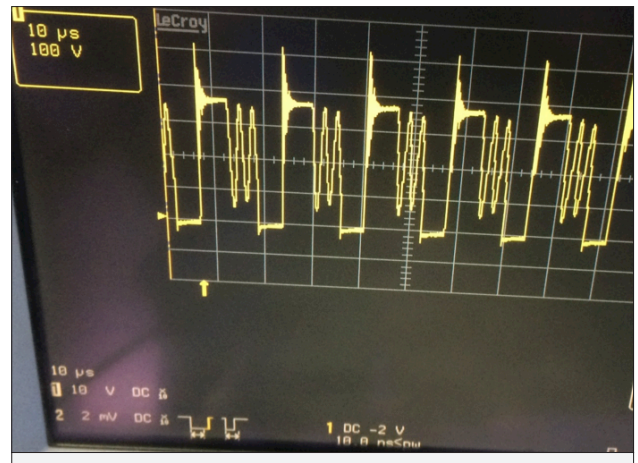


Figure 7. Power-switch voltage waveform



Figure 5. Input real and apparent power with PF values

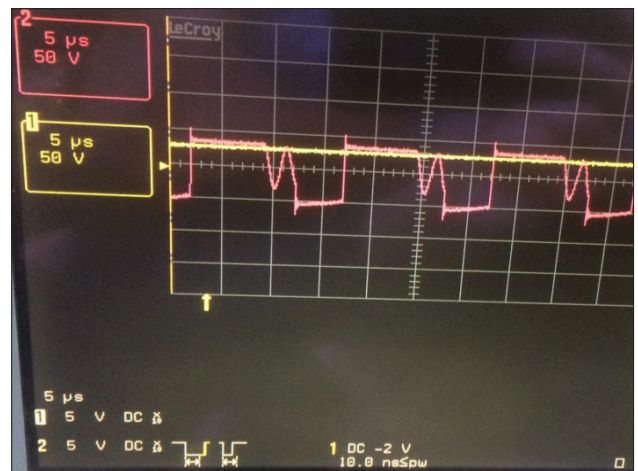


Figure 8. Output-diode voltage and current waveforms

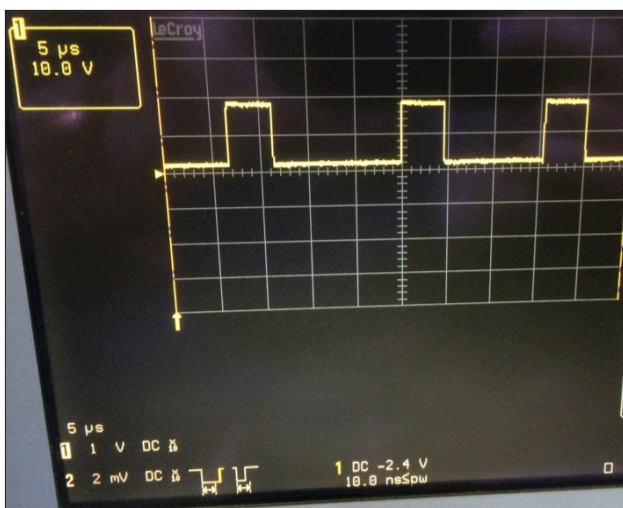


Figure 6. Power switch control signal waveform

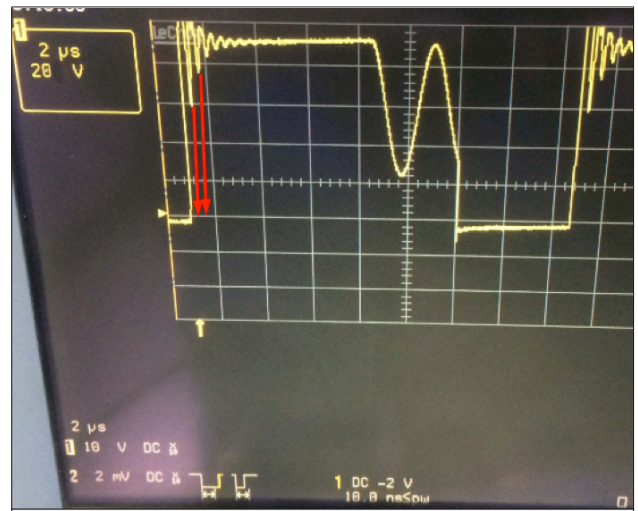


Figure 9. Output-diode snubber circuit calculation point

In Figure 5, the real and apparent power values with PF value can be seen. The output power is measured to be 10.5 W and the real power 13.85 W. Therefore, the efficiency of the converter is calcu-

lated to be 75.8 %. At that time, the PF is measured to be 0.986, which is far from the unity point. The control signal is depicted in Figure 6 with the switching frequency equal to 69 kHz.

The power-switch voltage waveform is depicted in Figure 7. The peak voltage is approximately 525 V, which is the sum of the input voltage and reflected output voltage. To lower the reflected output voltage, a zener diode and serial diode are connected to the primary side of the transformer. The aim of the zener diode is to trim the output reflected voltage above 170 V. The zener-and-diode-combination circuit is called the clamp circuit. For withstanding the peak voltage of 800 V, the STD4NK80ZT4 mosfet is used. To reduce the voltage stress on the power switch, a snubber circuit is connected. The output power-diode voltage and current waveforms are depicted in Figure 8.

Snubber Circuits

The flyback most important energy transfer parts are the power switch and output power diode. The voltage stresses on the output diode and the power switch result in extra power losses, lowering the efficiency. The proposed snubber circuit comprises resistive and capacitive elements. To calculate the power-diode snubber R and C values, first the power-diode ring period, T_r , must be measured. The measurement is depicted in Figure 9. The value of T_r is measured to be 50 ns. After calculation, the C_{sn1} value is selected to be 0.47 nF.

R_{sn1} is calculated to be 51 Ω using equation (11). The power loss corresponding to this resistance is calculated to be 329 mW using equation (12). One has the following:

$$R_{sn1} = \frac{3T_r}{2\pi C_{sn1}} = \frac{3 * 50ns}{2 * \pi * 0,47nF} = 51\Omega \quad (11)$$

$$P_{RSNB} = C_{sn1} * V_{IN} * f_r = C_{sn1} * V_{sek} * \frac{1}{T_r} = 0,47nF * 35 * \frac{1}{50ns} = 0,329W \quad (12)$$

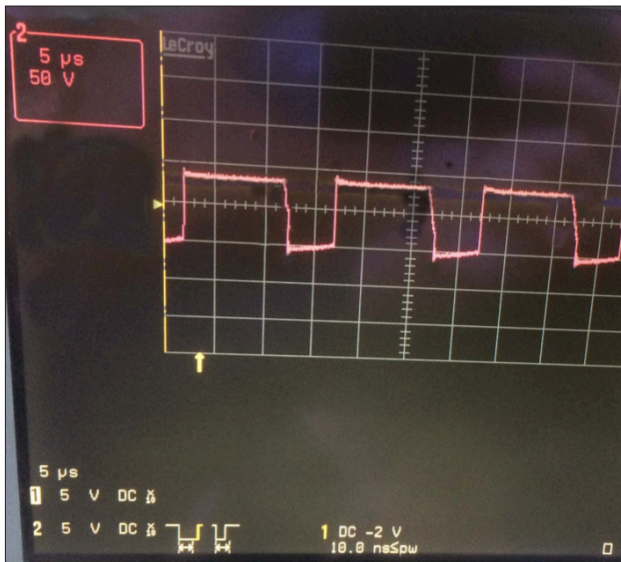


Figure 10. Output-diode voltage waveform with added snubber circuit

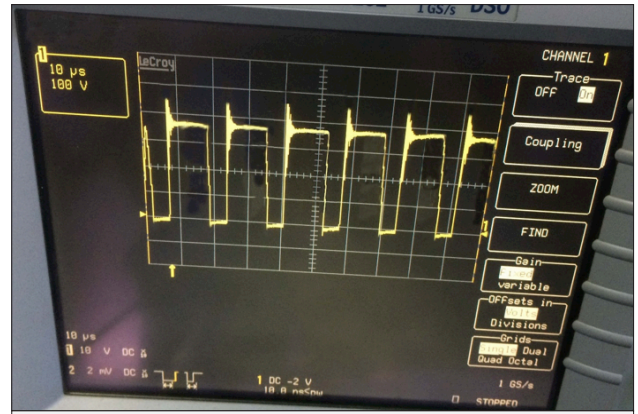


Figure 11. Power-switch voltage waveform with added snubber circuit

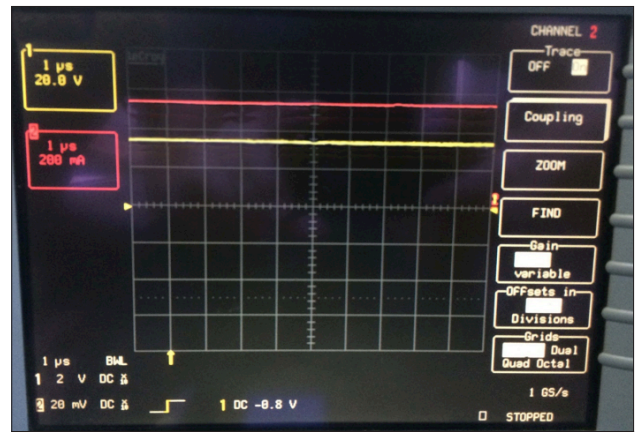


Figure 12. Output voltage and current waveforms with the added snubber circuit

Finally, the calculated snubber R and C components are added to the output power diode to achieve better voltage waveforms. Although in Figure 8, the output power-diode voltage stress is higher than 100V, in Figure 10, this voltage stress is dropped dramatically to 90 V without fluctuation.

Generally, SMPS circuits operate at high frequencies to reduce the cost. The high frequencies result in repetitive voltage stresses on the power switch. Furthermore, a high switching frequency results in noise and switching power loss. This switching power loss reduces the converter efficiency.

In equation (13), P_{sn2} is calculated to be 16 mW. According to equations (14) and (15), R and C snubber components are calculated to be R_{sn2} as 45 k Ω and C_{sn2} as 0.32 nF, respectively. One has the following:

$$P_{sn2} = \frac{1}{2} I_{lk} I_s^2 f_s = \frac{1}{2} * 45uH * 0.1^2 * 69kHz = 0.016W \quad (13)$$

$$R_{sn2} = \frac{V_{sn}^2}{P_{sn}} = \frac{213^2}{0.016} = 45k\Omega \quad (14)$$

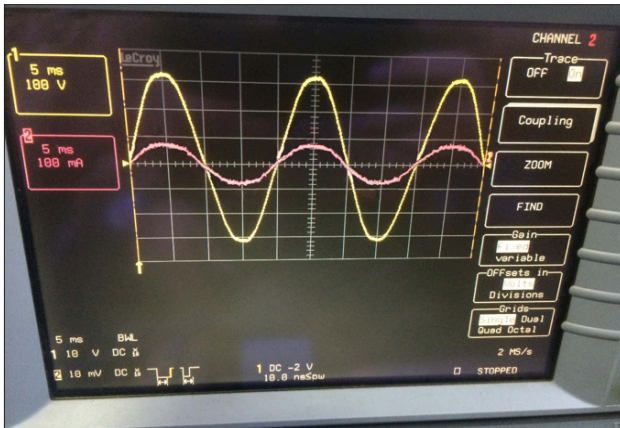


Figure 13. Input voltage and current waveforms with the added snubber circuit

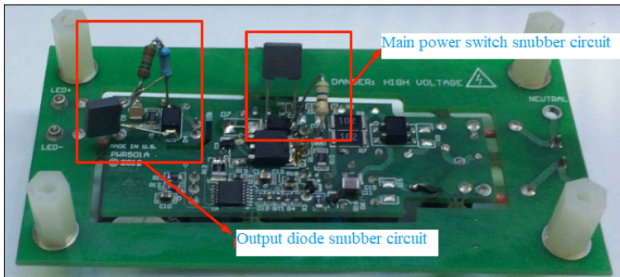


Figure 14. Added snubber circuits

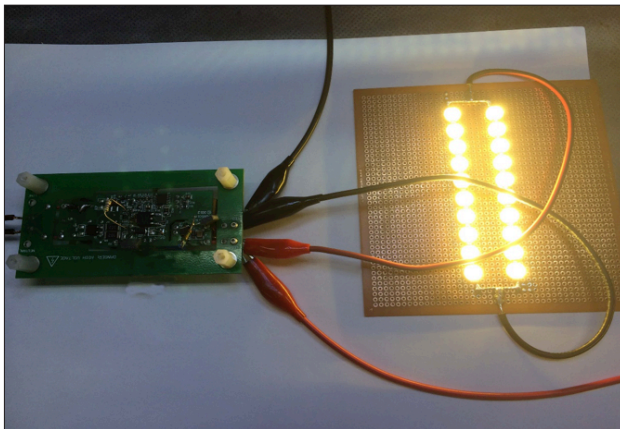


Figure 15. Experimental setup

$$C_{sn2} = \frac{1}{f_s R_{sn2}} = \frac{1}{69kHz * 45k\Omega} = 0,32nF \quad (15)$$

A commercially available 0.47-nF, 300-V capacitor was chosen as the Csn2 capacitor with UF4007 fast diode. After adding the snubber circuit, the measurements were taken again. Although in Figure 7, the power-switch voltage stress is higher than 525V, in Figure 11, this voltage stress is dropped dramatically to 460 V without fluctuation.

According to the voltage waveform depicted in Figure 11, the voltage stress is decreased. Therefore, this reduction in the voltage stress increases the efficiency. To see the improvement upon using the proposed topology, the output voltage and current waveforms are taken again in Figure 12. Furthermore, the improvements can be seen in Figure 13 with the input voltage and current waveforms. The voltage and current waveforms are not only sinusoidal but also in the same phase, thereby resulting in unity PF.

The experimental application circuit is depicted in Figure 14 with the snubber circuits. Furthermore, the working application is depicted in Figure 15 as an LED driver.

Conclusion

Particularly, in the last 10 years, research works have boosted the LED technology, covering almost the entire lighting sector. In this study, LED driver circuits in the literature were discussed. The advantages and disadvantages of these circuits are examined for isolation, PFC, and efficiency. The application of the PAR230VEM flyback LED driver circuit is analyzed, and less PF, high voltage stresses, and high switching power losses are noticed. Although flyback converters provide isolation for low-power LED drivers, owing to the high switching frequency, the consequent voltage stresses lower the efficiency. To overcome these drawbacks, snubber circuits are added to the power diode and power switch. Consequently, the proposed topology provides not only isolation and unity PF for LED drivers but also high efficiency. Finally, the efficiency is improved by 9.4 % with 4.8 % THDi at the switching frequency of 69 kHz.

Peer-review: Externally peer-reviewed.

Conflict of Interest: The author have no conflicts of interest to declare.

Financial Disclosure: The author declared that the study has received no financial support.

References

1. C. B. Park, B. H. Choi, J. P. Cheon, C. T. Rim, "Robust active LED driver with high power factor and low total harmonic distortion compatible with a rapid-start ballast", *J Power Electron*, vol. 14, no. 2, pp. 226-36, Mar, 2014. [CrossRef]
2. E. M. Sá, C. S. Postiglione, F. L. M. Antunes, A. J. Perin, "Low cost ZVS PFC driver for power LEDs", 35th Annual Conference of IEEE Industrial Electronics, Porto, 2009, pp. 3551-6.
3. T. Chern, T. Huang, W. Wu, W. Lin, G. Hwang, "Design of LED driver circuits with single-stage PFC in CCM and DCM", 6th IEEE Conference on Industrial Electronics and Applications, Beijing, 2011, pp. 2358-63. [CrossRef]
4. B. Singh, A. Shrivastava, A. Chandra, K. Al-Haddad, "A single stage optocoupler-less buck-boost PFC driver for LED lamp at universal AC mains", IEEE Industry Applications Society Annual Meeting, Lake Buena Vista, FL, 2013, pp. 1-6. [CrossRef]
5. A. Mohamadi, E. Afjei, "A single-stage high power factor LED driver in continuous conduction mode", The 6th Power Electronics, Drive Systems & Technologies Conference (PEDSTC2015), Tehran, 2015, pp. 462-7. [CrossRef]

6. Q. Zheng, W. Lin, Y. Xu, L. Wang, N. Wu, "Research on a novel constant power control strategy for single-stage PFC LED driver", 11th China International Forum on Solid State Lighting (SSLCHINA), Guangzhou, 2014, pp. 5-8. [\[CrossRef\]](#)
7. B. Poorali, E. Adib, "Analysis of the Integrated SEPIC-Flyback Converter as a Single-Stage Single-Switch Power-Factor-Correction LED Driver", in IEEE Transactions on Industrial Electronics, vol. 63, no. 6, pp. 3562-3570, Jun, 2016. [\[CrossRef\]](#)
8. R. L. dos Santos, R. P. Coutinho, K. C. A. de Souza, E. M. Sá, "A dimmable charge-pump ZVS led driver with PFC", 2015 IEEE 13th Brazilian Power Electronics Conference and 1st Southern Power Electronics Conference (COBEP/SPEC), Fortaleza, 2015, pp. 1-6. [\[CrossRef\]](#)
9. T. Alunpipatthanachai, S. Bhatranand, C. Jeraputra, "Design of a single stage PFC LED driver with a leakage energy recycling circuit", 13th International Conference on Electrical Engineering/Electronics, Computer, Telecommunications and Information Technology (ECTI-CON), Chiang Mai, 2016, pp. 1-6. [\[CrossRef\]](#)
10. B. Poorali, E. Adib, H. Farzanehfard, "A Single-Stage Single-Switch Soft-Switching Power-Factor-Correction LED Driver", in IEEE Transactions on Power Electronics, vol. 32, no. 10, pp. 7932-40, Oct, 2017. [\[CrossRef\]](#)
11. S. M. Ferdous, M. A. M. Oninda, G. Sarowar, K. K. Islam, M. A. Hoque, "Non-isolated single stage PFC based LED driver with THD minimization using Cúk converter", 9th International Conference on Electrical and Computer Engineering (ICECE), Dhaka, 2016, pp. 471-4. [\[CrossRef\]](#)
12. A. R. Saxena, A. Kulshreshtha, "Universal bus front end PFC fourth-order buck converter as LED drivers", TENCON 2017 - 2017 IEEE Region 10 Conference, Penang, 2017, pp. 1755-60. [\[CrossRef\]](#)
13. Y. Liu, F. Syu, H. Hsieh, K. A. Kim, H. Chiu, "Hybrid Switched-Inductor Buck PFC Converter for High-Efficiency LED Drivers", in IEEE Transactions on Circuits and Systems II: Express Briefs, vol. 65, no. 8, pp. 1069-73, Aug, 2018. [\[CrossRef\]](#)
14. R. L. dos Santos, D. M. Rufino, M. B. M. de Moraes, E. M. Sá, "A charge-pump led driver with PFC and low-frequency-flicker reduction", Brazilian Power Electronics Conference (COBEP), Juiz de Fora, 2017, pp. 1-7. [\[CrossRef\]](#)
15. H. S. H. Chung, W. Cheung, K. Tang, "A ZCS bidirectional flyback converter", IEEE 35th Annual Power Electronics Specialists Conference (IEEE Cat. No.04CH37551), Aachen, Germany, 2004, pp. 1506-12.
16. T. E. Salem, W. Tipton, D. Porschet, "Fabrication and Practical Considerations of a Flyback Transformer for Use in High Pulsed-Power Applications", Proceeding of the Thirty-Eighth Southeastern Symposium on System Theory, Cookeville, TN, 2006, pp. 406-9.
17. X. Zhang, H. Liu, D. Xu, "Analysis and design of the flyback transformer", in IECON'03. 29th Annual Conference of the IEEE Industrial Electronics Society (IEEE Cat. No. 03CH37468), IEEE, vol. 1, 2003, pp. 71-9.
18. J. Noon, "UC3855A/B High Performance Power Factor Preregulator", Texas Instruments Application Report, Apr, 2004
19. S. Park, S. Choi, "Soft-Switched CCM Boost Converters With High Voltage Gain for High-Power Applications", in IEEE Transactions on Power Electronics, vol. 25, no. 5, pp. 1211-7, May 2010. [\[CrossRef\]](#)
20. C. M. Wang, "A novel zero-Voltage-switching PWM boost rectifier with high power factor and low conduction losses", in IEEE Transactions on Industrial Electronics, vol. 52, no. 2, pp. 427-35, Apr, 2005. [\[CrossRef\]](#)
21. Y. Jang, M. M. Jovanovic, K. Fang, Y. Chang, "High-power-factor soft-switched boost converter", in IEEE Transactions on Power Electronics, vol. 21, no. 1, pp. 98-104, Jan, 2006. [\[CrossRef\]](#)
22. B. Akin, H. Bodur, "A New Single-Phase Soft-Switching Power Factor Correction Converter", in IEEE Transactions on Power Electronics, vol. 26, no. 2, pp. 436-43, Feb, 2011. [\[CrossRef\]](#)
23. B. Akin, "An Improved ZVT-ZCT PWM DC-DC Boost Converter With Increased Efficiency", in IEEE Transactions on Power Electronics, vol. 29, no. 4, pp. 1919-26, Apr, 2014. [\[CrossRef\]](#)



Burak Akin was born in Istanbul, Turkey, in 1977. He received the B.S., M.S., and Ph.D. degrees in electrical engineering from Yildiz Technical University, Istanbul, Turkey, in 1998, 2001, and 2008, respectively. From 1999 to 2013, he was a research assistant in the Department of Electrical Engineering, Yildiz Technical University. Since September 2013, he has been working as an assistant professor at the same department. He has authored or coauthored more than 50 journal and conference papers in the area of power electronics. He was also engaged in four research projects involving power electronics. His current research interests include power-factor correction, switching power supplies, high-frequency power conversion, and active and passive snubber cells in power electronics.